Catalysis Today 158 (2010) 63–68

Contents lists available at ScienceDirect

Catalysis Today

journal homepage: www.elsevier.com/locate/cattod

In situ sum frequency generation vibrational spectroscopy study of CO adsorption on Au surfaces promoted by Ar^+ sputtering and FeO_x additives

O. Hakkel[a], Z. Pászti[a], A. Berkó[a,b], K. Frey[c], L. Guczi[a,c,*]

[a] Chemical Research Center, Institute of Nanochemistry and Catalysis, Hungarian Academy of Sciences, P.O. Box 17, H-1525 Budapest, Hungary
[b] University of Szeged, Department of Physical Chemistry and Material Science, P.O. Box 168, H-6701 Szeged, Hungary
[c] Institute of Isotopes, Hungarian Academy of Sciences, P.O. Box 77, H-1525 Budapest, Hungary

ARTICLE INFO

Keywords:
CO adsorption
CO oxidation
Gold/oxide interface
Inverse catalysis

ABSTRACT

Identification of the active sites is a key factor in understanding the mechanism of gold-catalyzed reactions. In this work we investigated the CO adsorption properties of gold-based model catalysts ranging from native and surface-modified single crystal surfaces to polycrystalline thin films promoted by iron oxide layers. The results, completed with those obtained on a gold nanoparticle-containing system, clearly demonstrate the role of the defect sites in the CO adsorption. In addition, a promoter such as iron oxide can further enhance CO adsorption, probably through a mechanism connected to the interface formation between gold and iron oxide.

1. Introduction

Detailed understanding of the processes occurring at interfaces between solid materials and their environment is a key factor in the design of novel functional materials. Until recently, the well-established tools of traditional surface science requiring ultrahigh vacuum environments have been employed to establish this understanding. On the other hand, most functional materials are intended for use under atmospheric pressures or even in aqueous environments, therefore a "pressure gap" exists between the needs of the practical materials engineering and the knowledge about the interfacial behavior of these materials [1]. In addition, practical functional materials are multi-component systems with often very complicated micro- and nanostructure, while information on fundamental surface chemical processes is typically gathered by studying simple and very well defined models like single crystal surfaces, which creates a "materials gap". Accordingly, one of the most exciting areas of modern surface science comprises efforts aimed at bridging these gaps by introducing novel probes for *in situ* or *in operando* characterization of model systems with ever increasing complexity.

Sum frequency generation vibrational spectroscopy (SFG), a spectroscopic tool based on a second order nonlinear optical effect, offers excellent opportunities for molecular level investigation of surface chemical processes under realistic conditions. As the result of its inherent surface specificity and sub-monolayer sensitivity, the method is capable for studying interfacial phenomena at gas–solid, liquid–solid and even liquid–liquid interfaces [2–5]. A pioneering SFG study of gas adsorption on supported nanoparticles was published by Rupprechter and co-workers [1]. They measured CO adsorption on Pd nanoparticles and thereby could identify the bonding structures and geometry of adsorbed CO molecules.

For fundamental understanding of catalysis by gold, well defined gold surfaces may provide useful information concerning reaction mechanisms and the nature of active centers. A very recent paper by Nieuwenhuys has made an excellent summary on CO chemisorption on Au single crystal surfaces [6]. Both experimental and theoretical results are discussed in this work. A large difference between the flat Au(1 1 1), by far the most studied surface, and stepped/kinked surfaces, is found, demonstrating the importance of low-coordinated Au atoms for high catalytic activity [7].

Gottfried et al. [8] reported that additional high temperature CO desorption peaks appear after sputtering an Au(1 1 0) surface, indicating that CO adsorbs more strongly on defects, i.e. atoms with a coordination number below seven. Comparison with literature, the results showed that the CO adsorption energy is not only dependent on the coordination number of the Au atoms, but the exact geometrical structure of the surface also plays a role. Piccolo et al. [9] studied the adsorption of CO on Au(1 1 1) in the 10^{-3}–10^{3} mbar range at room temperature. Using scanning tunneling microscopy (STM), a CO-induced modification of the surface morphology (step edge roughening) and terrace structure is evidenced.

Extrapolation of these results to supported gold catalysts is, however, not straightforward. For example, there is no unambiguous clarification about the site at which the CO molecules can be activated. When the gold particle size is in the nano range (2–6 nm), CO can be chemisorbed on the metallic gold particles, although the

* Corresponding author at: Institute of Isotopes, HAS, P.O. Box 77, H-1525 Budapest, Hungary. Tel.: +36 1 392 2534; fax: +36 1 392 2703.
E-mail addresses: guczi@mail.kfki.hu, guczi@sunserv.kfki.hu (L. Guczi).

0920-5861/$ – see front matter © 2010 Published by Elsevier B.V.
doi:10.1016/j.cattod.2010.05.039

valence state is questionable. On large gold particles ($d > 15$ nm), no CO chemisorption occurs because the adsorption process is highly endothermic. It is, therefore, more plausible to assume that the gold/support interface along the perimeter of the gold particle serves as the adsorption site. In our previous studies it has been established that the Au/oxide interface plays a prevailing role in the CO oxidation both in model Au/FeO_x and in "inverse" FeO_x/Au [10,11] systems. It was suggested that the CO activation occurred at the perimeter of the gold/oxide interface.

Current research efforts in our laboratory are focused on model studies of gold catalysis by comparing the behavior of carbon-monoxide on systems of increasing complexity ranging from single crystals to supported nanoparticles. We developed a very promising experimental setup by connecting a SFG spectrometer to a multi-technique surface analytical system via an appropriately designed chamber capable for experiments at elevated pressures in a broad temperature range. This complex instrument allows sample preparation and characterization according to the standards of traditional surface science as well as *in situ* determination of the gas adsorption and transformation properties of the sample at ambient pressure. In the setup the sample is not exposed to air between preparation, characterization and SFG measurement, thus its surface composition and electronic structure can be unambiguously related to its gas adsorption properties.

In the present contribution we will summarize our observations made by this apparatus on CO adsorption over native and surface-modified Au(1 1 1) single crystals as well as gold-supported iron oxide thin films. The results will be discussed in comparison with data obtained on model systems containing gold nanoparticles.

2. Experimental

2.1. Sample preparation

The Au(1 1 1) single crystal was purchased from MaTeck GmbH (Germany) and was cleaned in the surface analysis system by repeated cycles of 2–3 keV Ar^+ sputtering and annealing until no contaminants were detected by XPS and the characteristic UPS spectrum of Au(1 1 1) was obtained. Scanning tunneling microscopy (WA Technology, United Kingdom) measurements carried out in a separate instrument confirmed the herringbone reconstruction of the surface after this treatment.

Gold thin film samples were evaporated by molecular beam epitaxy (MBE) technique, using an instrument from MECA-2000 (France). The Au layer was deposited on a 300 nm SiO_2-covered 2 in. Si(1 0 0) wafer at 4.1×10^{-9} mbar. The Au was evaporated using a high temperature (HT) effusion cell, from a graphite crucible. The evaporation temperature was 1480 °C, and the deposition rate was 0.178 Å/s. The thickness of the gold film was 20 nm. The gold film was cleaned by cyclic argon ion bombardment treatments (3 keV, 10 min) in the analytical chamber of the UHV system at room temperature. The cleanliness of the surface was checked by UPS and XPS measurements. Iron oxide layers were formed on the cleaned Au/SiO_2/Si support by electron beam evaporation from an iron rod in 4×10^{-7} mbar O_2 at room temperature. The layers were characterized by XPS and UPS measurements. After cleaning and iron oxide deposition the samples were transferred to the UHV-high pressure cell under ultrahigh vacuum conditions. The cleanliness of both the bare Au and the iron oxide surface was confirmed by the lack of C–H related vibrations (around 2920 cm^{-1}, not shown) in the SFG spectra.

For the CO oxidation test reaction more samples with thicker iron oxide layer were prepared by depositing 10 nm Fe on the top of the 20 nm Au film by electron gun. Iron oxide was formed by oxidation of the Fe film in air.

2.2. The surface analytical apparatus

The experimental work has been carried out in a system based on a sum frequency spectrometer made by EKSPLA (Vilnius, Lithuania). The visible beam (532 nm) used for the SFG studies is generated by doubling the fundamental output of a Nd:YAG laser (1064 nm wavelength, 20 ps pulse width, 20 Hz repetition rate) in a harmonics unit. The tunable IR beam is obtained from an optical parametric generation/difference frequency generation system. The beam energies at the sample vary from 10 to 250 μJ. Sum frequency light is collected in the reflected direction through a holographic notch filter and monochromator, and detected by a photomultiplier. Spectral resolution is determined by the ~6 cm^{-1} line width of the IR pulse. The spectrometer is completed with two sample stages: one exposed to atmospheric conditions and one housed in the UHV-high pressure cell of the surface analytical system.

The surface analytical system manufactured by Omicron Nanotechnology GmbH (Germany) consists of three chambers. The analytical chamber is equipped with an electron beam evaporation source and a fine focus ion gun for sample preparation, an EA 125 type hemispherical energy analyzer, a dual-anode X-ray source and a gas discharge lamp for X-ray and ultraviolet photoelectron spectroscopy. The vital part of the system is the dedicated SFG chamber, in which experiments can be performed from ultrahigh vacuum (better than 5×10^{-10} mbar) to atmospheric pressures. The sample temperature can be varied between 150 and 600 K. Laser beams necessary for SFG measurements are introduced into the chamber via large CaF_2 windows. The chamber is equipped with a gas manifold, and a Pfeiffer (Germany) made Prisma mass spectrometer. Further sample preparation tools can be attached to the preparation chamber. Fast and precise sample handling is facilitated by a load-lock system and two manipulators.

Test reaction for CO oxidation was performed in an all-glass circulation reactor connected to an ExTorr type quadrupole mass spectrometer via a capillary leak.

3. Results and discussion

Although both structural properties and working conditions of the supported gold catalysts significantly differ from those of model systems based on single crystals or thin films, fundamental aspects of gold catalysis may be understood by studying well defined model systems. Introduction of either structural or compositional complexity to a simple model is expected to reveal details about the mode of the adsorption of the reactants and the reaction mechanism itself. This is particularly true for carbon-monoxide oxidation by gold-based catalysts where the nature of the active site is still somewhat controversial. Accordingly, we will first present our results concerning on CO adsorption on single-crystalline gold, followed by a short description of studies on gold-supported iron oxide layers. The findings will be compared to results obtained on model systems containing gold nanoparticles.

3.1. CO adsorption on Au(1 1 1)

It is generally agreed that atomically smooth Au(1 1 1) surfaces interact very weakly with CO under conditions accessible in UHV-based surface analysis instruments [6]. Indeed, our own SFG measurements covering a broad pressure and temperature range (170–300 K, 10^{-7}–1 mbar) revealed no signs of CO adsorption on this surface.

On the contrary, Au(1 1 1) surfaces modified by Ar^+ ion bombardment readily adsorb carbon-monoxide, as evidenced by the SFG spectra presented in Fig. 1. Spectra up to 10^{-4} mbar CO pres-

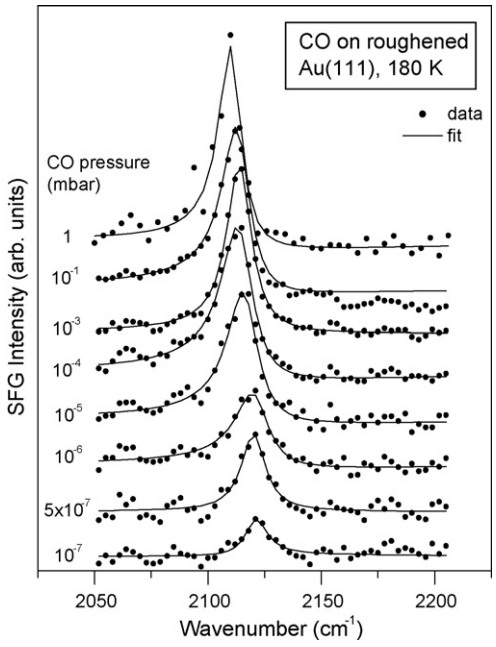

Fig. 1. SFG spectra of CO adsorbed on Au(1 1 1) roughened by 10 min 3 keV Ar^+ ion bombardment. Spectra were taken at 180 K in *ppp* polarization combination at pressures indicated in the graph. Traces are shifted vertically for clarity.

sure were taken in gas flow, while the ones above 10^{-4} mbar were measured under static conditions. All data were collected at 180 K sample temperature.

The SFG spectrum is essentially a vibrational spectrum of the surface adsorbates complicated by interference between the resonant peak(s) and the nonresonant background (which is the spectral contribution invariant with respect to the tuning of the infrared excitation). Parameters like frequency, strength and width of the resonant peaks can provide information about the nature of the bonding, properties of the adsorption sites as well as the quantity and/or orientation of the adsorbates [3,4]. According to the general theory of SFG from adsorbates on metal surfaces, these quantities can be deduced by fitting the spectra to the following formula [12,13]:

$$S(\omega_2) = \left| A_{\mathrm{NR}} + \sum_m \frac{A_m e^{i\varphi m}}{\omega_2 - \omega_m + i\Gamma_m} \right|^2$$

where $S(\omega_2)$ is the spectrum measured as the function of the frequency ω_2 of the infrared excitation, A_{NR} is the amplitude of the nonresonant contribution, and A_m, ω_m, Γ_m and φ_m are the amplitude, frequency, width and phase of the mth resonant mode, respectively. During spectrum processing, all parameters of the formula were varied until a satisfactory fit was achieved.

Fitting revealed that at all pressures studied here a single narrow (Γ = 6–8 cm^{-1}) Lorentzian peak sufficiently describes the measured signal. Furthermore, the line width value close to our experimental resolution suggests the lack of inhomogeneous broadening, thus it can be concluded that CO adsorbs at structurally very similar sites. The apparent asymmetry of the resonances is due to the interference between the resonant CO signal and the strong nonresonant contribution of the Au surface.

According to our observations, no adsorption was detected below 10^{-7} mbar CO pressure. The vibration frequency for the initial adsorbates (10^{-7} mbar) was found at 2121 cm^{-1}, which gradually shifted towards lower wavenumbers with increasing CO pressure (2110 cm^{-1} at 1 mbar). The adsorbates were rather unstable at the surface: evacuation of the chamber resulted in the immediate disappearance of the CO signal, regardless to the prior pressure.

Sum frequency spectra taken at different polarization combinations of the exciting laser beams and the signal provide data about the different elements of the second order nonlinear susceptibility tensor of the surface, which in turn can be used to deduce information on the orientation of the adsorbates [3,4]. Comparison of spectra measured in the *ppp* (all beams *p*-polarized, Fig. 1) and *ssp* (SFG signal and visible excitation *s*-polarized, infrared excitation *p*-polarized, not shown here) combinations suggest no major orientation change with respect to variation of the CO pressure. Since the SFG signal is simultaneously sensitive for the orientation and surface density of the adsorbates [4], the pressure dependent change of the signal intensity can be directly related to the change in the adsorbed CO amount.

The observed vibration frequency and its change with increasing CO exposure is in very good agreement with the results obtained on other Au surfaces as (1 1 0) which readily adsorbs CO even at room temperature [14,15], (3 3 2) which is characterized by narrow (1 1 1) terraces separated by monatomic steps [16] or even supported Au nanoparticles [17,18], thus the signal can safely be assigned to CO molecules adsorbed on Au atoms in on-top position. The exposure-dependent shift is attributed to the combined effects of dipole–dipole interaction, which tends to increase the observed vibrational frequency and the chemical shift which reflects changes in the bonding of the CO molecules as the coverage is increased [17].

In experiments performed on roughened Au(1 1 1) surfaces prepared similarly to those studied here [19] CO exposures up to a few Langmuirs at temperatures below 120 K resulted in stable adsorbates showing the same shift in the CO frequency as found in the present work. Nevertheless, TPD studies revealed that all CO desorbed at temperatures below 180–200 K, i.e. in the range of the lowest temperatures investigated by us. Therefore, it can be stated that above the temperature range of the stable adsorbates a second adsorption regime exists in which CO is bound probably at very similar sites but in a more dynamic manner provided the CO pressure is sufficiently high.

The enhanced affinity of CO towards the ion bombarded surface suggests that the morphology may have been significantly altered. Therefore, scanning tunneling microscopy studies were carried out in a separate UHV system, under identical sample preparation conditions as used for the gas adsorption experiments. Indeed, STM images confirmed that the ion bombardment drastically rearranged the surface (see Fig. 2).

Large, atomically smooth terraces were seen on the cleaned-annealed surface, with monatomic steps between the terraces. The corrugation (height difference between the highest and lowest point of the imaged surface) was 1.1 nm. The ion bombardment completely destroyed the terraces. Instead, a pit and mound-like structure was created, with holes as deep as 6–8 atomic layers and with protrusions of nearly the same height, which is reflected in the increased corrugation value (4.6 nm). These images were chosen from 20 to 30 records of different sizes taken up on several regions of the sample. It is important to note that the variation of the surface corrugation for the two cases separately (naturally for a given image size) was not more than 15%, subsequently, the approximately 4-fold increase in the corrugation is a clear and unambiguous indication for the changed terrace structure. Furthermore, the structural changes are qualitatively similar to that observed in Ref. [19] under similar preparation conditions.

The STM images reveal that the ion bombardment very significantly increased the density of steps, while the typical terrace width was considerably reduced, especially at the side walls of the pits and mounds. Taking into account that line width data suggested only one type of adsorption site, CO is proposed to adsorb at the step edge atoms. It is worth to note that the low density of the

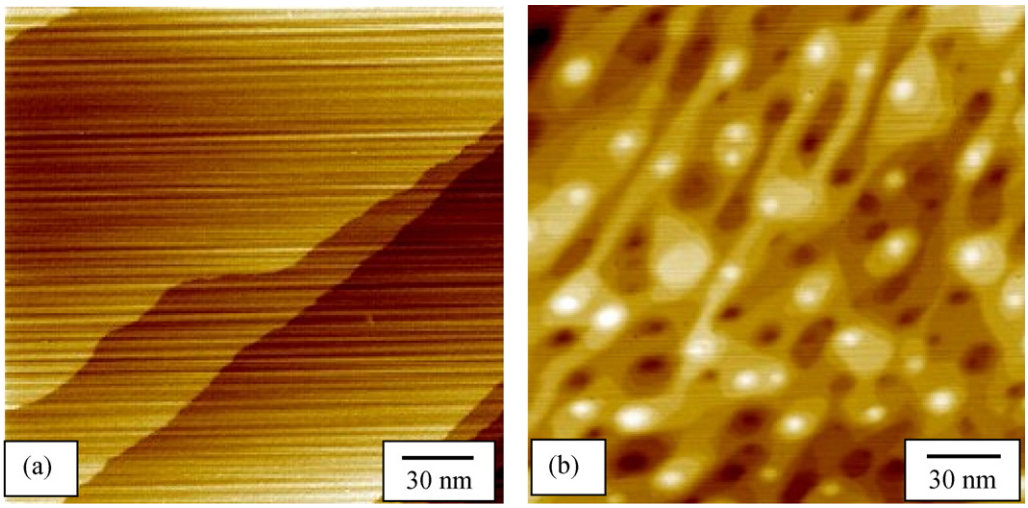

Fig. 2. 200 nm × 200 nm STM image of (a) the cleaned and annealed Au(1 1 1) surface and (b) the same surface after 10 min 3 keV Ar^+ ion bombardment. The *z*-scale can be derived from the corrugation (height difference between the highest and lowest point of the imaged surface corresponding to the brightest and darkest spots), which was 1.1 nm in (a) and 4.6 nm in (b).

steps separating the wide terraces of the cleaned-annealed surface limits the concentration of the CO adsorbates to levels below our detection limit.

A detailed sum frequency and electron spectroscopy study of CO adsorbates is still in progress in our laboratory; the corresponding results will be published elsewhere.

3.2. CO adsorption on gold-supported iron oxide thin films

In a separate set of experiments the influence of an iron oxide layer was investigated on the CO adsorption properties of gold.

An MBE-grown polycrystalline Au film was used as substrate. Iron oxide layers of 2 and 8 nm thickness as estimated from the quantitative evaluation of the intensities of the Fe, O and Au photoelectron lines were deposited onto the Au substrate in our surface analytical system. The Fe 2p spectra of the films are presented in Fig. 3, along with reference spectra from Fe_2O_3 powder (containing Fe^{3+} states) and a thick film deposited under reduced oxygen partial pressure (containing mostly Fe^{2+} ions with some Fe^{3+} states). Inspection of the spectra reveals that the Au-supported iron oxide films always contain a mixture of Fe^{3+} and Fe^{2+} states, the thinner film being slightly more Fe^{2+}-richer than the thicker one. Evaluation of the Fe:O ratios confirms this finding, while indicates that both films are rather oxygen-deficient: for the 2 nm layer 1:0.8, while for the 8 nm one 1:1.1 ratio was found. X-ray diffraction data proved that both films are amorphous.

SFG results for CO interaction with the 2 nm iron oxide films are summarized in Fig. 4. Although the signal is rather weak and noisy, the pressure dependence of the CO derived feature around 2090–2100 cm^{-1} is evident. The derivative-like peak shape is due to the interference with the nonresonant background, which can be constructive (as in the case of the roughened Au(1 1 1) surface), destructive (which leads to appearance of negative peaks) or in between these extreme cases, depending on the phase relationship between the resonant signal and the background [20]. Due to this interference, the CO vibrational frequency was determined by fitting, which revealed a value around 2103 cm^{-1} in both cases. Temperature-dependent studies indicated that the structure due to adsorbed CO is present at least up to 210–220 K in 10 mbar CO [21]. It is worth to note that the vibrational frequency of CO on the 2 nm iron oxide covered gold sample shifts towards somewhat lower values with respect to that observed on pure gold.

On the contrary, we were unable to identify CO-related SFG signals in the spectra taken on the 8 nm FeO_x film covered Au sample. In addition, no CO adsorbates were found on the bare Au film in pressures up to 10 mbar [21], in good agreement with the lack of CO adsorption on the intact Au(1 1 1) surface (see above).

The relatively small amount of experimental information collected about the interaction of CO with iron oxides suggests no adsorption on oxygen terminated surfaces [22]. On the (1 1 1) surface of Fe_3O_4 grown on Pt(1 1 1) CO adsorbates were found to desorb in three peaks at 110, 180 and 230 K. The low temperature desorption peak with CO vibrational frequency around 2130 cm^{-1} was assigned to very weakly bound, mobile carbon-monoxide species, while the 180 and 230 K peaks with frequencies at 2080 and 2207 cm^{-1} were attributed to adsorbates bonded to Fe^{2+} sites on terraces and exposed Fe^{3+} sites at step edges, respectively [22].

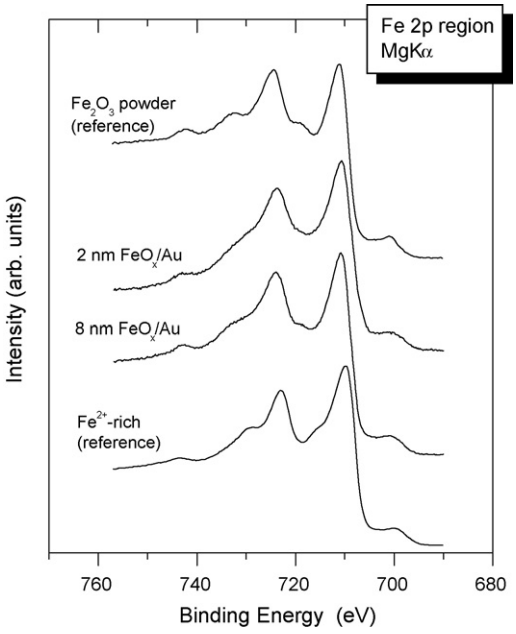

Fig. 3. Fe 2p core level spectra of the 2 and 8 nm iron oxide films deposited on MBE-grown gold. The spectra of a Fe_2O_3 powder sample and an evaporated thin film containing predominantly Fe^{2+} species are also presented for reference.

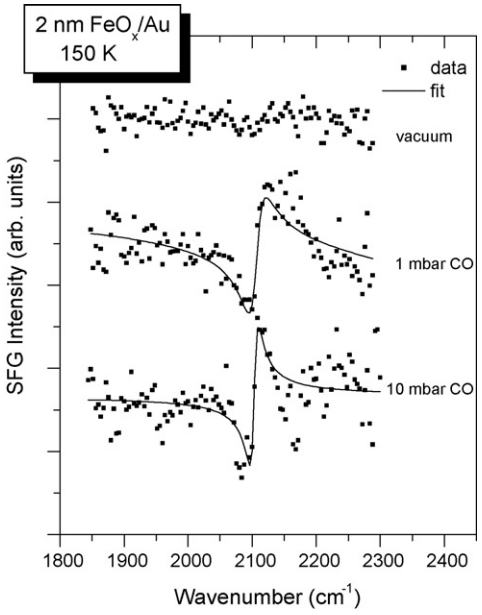

Fig. 4. SFG spectra of the CO stretching region for 2 nm iron oxide film deposited on gold at 150 K at different CO pressures. For reference, the spectrum measured in vacuum is also shown. Spectra were taken in the *ppp* polarization combination.

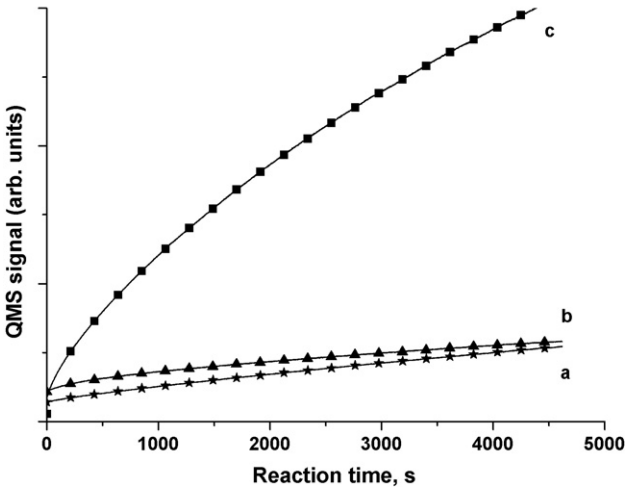

Fig. 5. Activity vs. reaction time for CO oxidation over 300 nm SiO_2/Si(1 0 0) (a), 10 nm FeO_x/300 nm SiO_2/Si(1 0 0) (b) and 10 nm FeO_x/20 nm Au/300 nm SiO_2/Si(1 0 0) (c).

As the vibrational frequency of CO adsorbates on metallic iron was reported to be below 2055 cm^{-1} [23], Fe^0 sites can be excluded as potential CO adsorption sites for the iron oxide promoted Au films studied here. The 2080 cm^{-1} frequency of CO at Fe^{2+} sites is still too low, while the 2207 cm^{-1} value characteristic for adsorption at Fe^{3+} sites is too high to explain our data. On the other hand, the observed frequency value of 2103 cm^{-1} is only slightly smaller than those found for the sputtering modified Au(1 1 1) surfaces, therefore we believe that in the case of the 2 nm iron oxide film CO adsorbs on bare gold areas between the FeO_x patches, maybe along the gold-iron oxide perimeter. Indeed, Fe or iron oxide formed by subsequent oxidation of the Fe layer form island films on Au(1 1 1) at low coverages [24], leaving significant uncovered gold areas, which diminish as the nominal film thickness is increased. The lack of the CO signal from the 8 nm film may thus suggest the formation of a continuous iron oxide overlayer. Nevertheless, a systematic spectroscopic and morphological characterization of FeO_x covered Au(1 1 1) surfaces may offer further insight into the adsorption behavior of CO in the presence of thin iron oxide layers supported by gold; such investigations are in the focus of our current research efforts.

3.3. CO oxidation over the FeO_x/Au/SiO_2/Si(1 0 0) surface

In Fig. 5 the catalytic activity of the samples tested in the CO oxidation are presented. After 60 min treatment in 200 mbar H_2 at 573 K the samples were heated up to 803 K in vacuum, then a mixture of 9 mbar CO + 18 mbar O_2 + 153 mbar He was introduced. The 10 nm FeO_x/20 nm Au/300 nm SiO_2/Si(1 0 0) sample showed high activity in the CO oxidation reaction. The 300 nm SiO_2/Si(1 0 0), 10 nm FeO_x/300 nm SiO_2/Si(1 0 0) and 20 nm Au/300 nm SiO_2/Si(1 0 0) (not shown) samples were much less active.

3.4. Gold nanoparticles versus thin gold layer

Important information can be gained from a model system using well defined gold thin films deposited by thermal evaporation onto a Si(1 0 0) wafer covered by native SiO_2 of nanometer thickness. There are several examples published in the literature [25], but the most obvious results can be obtained when a SiO_2/Si(1 0 0) model system [26–28] has been used.

In these studies it was established that continuous Au films show very limited activity in CO oxidation, especially if they are not promoted with additional iron oxide layers. This observation is in obvious accordance with the lack of CO adsorption on either smooth Au(1 1 1) or MBE-grown Au film as reported above. A thin FeO_x film on the top of the Au layer facilitates CO adsorption, which is also reflected in the enhancement of the CO oxidation rate. On the other hand, introduction of defect (step edge and kink) sites very significantly increases CO adsorption even at elevated temperatures. As nanoparticles are expected to contain these defect sites, it is not surprising that they are more active in CO oxidation than smooth films. Nevertheless, Au nanoparticles in contact with iron oxide show the highest activity in CO oxidation, which should reflect itself in changes of the CO adsorption properties of iron oxide promoted roughened Au(1 1 1) surface. The experimental confirmation of this expected behavior is in progress in our laboratory.

4. Conclusion

On the basis of the experiments it can be established that the CO cannot be adsorbed on smooth gold surface, or single crystal. Once the surface is roughened by ion bombardment, that is some kinks, corners and especially edges are generated, CO can be adsorbed on those sites. On smooth gold surface the CO adsorption is not significantly enhanced even if a promoter, like iron oxide is present. Conversely, if the gold surface is uneven, a promoter can further enhance CO adsorption, such as if one moves from gold film to gold nanoparticles. Evidence derived from investigations of gold nanoparticles in contact with iron oxide suggests that the interface operates to enhance the CO adsorption.

Acknowledgements

The authors are grateful to F. Tanczikó for technical help in preparing the model samples by MBE. The help of T. Keszthelyi with the SFG measurements is gratefully acknowledged. The financial support of the Hungarian Science and Research Fund (OTKA) grant Nos. K69200, K68052 and NNF 78837, as well as the COST program (D36/006/2008) is acknowledged.

References

[1] T. Dellwig, G. Rupprechter, H. Unterhalt, H.-J. Freund, Phys. Rev. Lett. 85 (2000) 776–779.
[2] M.C. Yang, K.C. Chou, G.A. Somorjai, J. Phys. Chem. B 108 (2004) 14766–14779.
[3] Z. Chen, Y.R. Shen, G.A. Somorjai, Annu. Rev. Phys. Chem. 53 (2002) 437–465.
[4] G.L. Richmond, Annu. Rev. Phys. Chem. 52 (2001) 357–389.
[5] M.L. Clarke, J. Wang, Z. Chen, J. Phys. Chem. B 109 (2005) 22027–22035.
[6] A.C.S. Carabineiro1, E.B. Nieuwenhuys, Gold Bull. 42 (2009) 288–301.
[7] R. Meyer, C. Lemire, S.K. Shaikhutdinov, H. Freund, Gold Bull. 37 (2004) 72.
[8] J.M. Gottfried, K.J. Schmidt, S.L.M. Schroeder, K. Christmann, Surf. Sci. 536 (2003) 206–224.
[9] L. Piccolo, D. Loffreda, F. Aires, C. Deranlot, Y. Jugnet, P. Sautet, J.C. Bertolini, Surf. Sci. 566–568 (2004) 995–1000.
[10] L. Guczi, G. Pető, A. Beck, K. Frey, O. Geszti, G. Molnár, Cs. Daróczi, J. Am. Chem. Soc. 125 (2003) 4332–4337.
[11] L. Guczi, K. Frey, A. Beck, G. Pető, Cs. Daróczi, N. Kruse, S. Chenakin, Appl. Catal. A 291 (116–125) (2005).
[12] Z. Pászti, L. Guczi, Vibr. Spectroscopy 50 (2009) 48–56.
[13] Z. Pászti, J. Wang, M.L. Clarke, Z. Chen, J. Phys. Chem. B 108 (2004) 7779–7787.
[14] Y. Jugnet, F.J. Cadete Santos Aires, C. Deranlot, L. Piccolo, J.C. Bertolini, Surf. Sci. 521 (2002) L639–L644.
[15] C.D. Meier, V. Bukhtiyarov, D.W. Goodman, J. Phys. Chem. B 107 (2003) 12668–12671.
[16] C. Ruggiero, P. Hollins, Surf. Sci. 377–379 (1997) 583–586.
[17] J. France, P. Hollins, J. El. Spect. Rel. Phenom. 64–65 (1993) 251–258.
[18] C. Lemire, R. Meyer, Sh.K. Shaikhutdinov, H.J. Freund, Surf. Sci. 552 (2004) 27–34.
[19] W.-L. Yim, T. Nowitzki, M. Necke, H. Schnars, P. Nickut, J. Biener, M.M. Biener, V. Zielasek, K. Al-Shamery, M. Bäumer, J. Phys. Chem. C 111 (2007) 445–451.
[20] C.T. Williams, Y. Yang, C. Bain, Catal. Lett. 61 (1999) 7–13.
[21] O. Hakkel, Z. Pászti, T. Keszthelyi, K. Frey, L. Guczi, React. Kin. Catal. Lett. 96 (2009) 345–356.
[22] C. Lemire, R. Meyer, V.E. Henrich, Sh. Shaikhutdinov, H.J. Freund, Surf. Sci. 572 (2004) 103–114.
[23] T. Wadayama, K. Kubo, T. Yamashita, T. Tanabe, A. Hatta, J. Phys. Chem. B 107 (2003) 3768–3773.
[24] N.A. Khan, C. Matranga, Surf. Sci. 602 (2008) 932–942.
[25] (a) M. Haruta, Cattech 6 (2002) 102–115;
(b) S.H. Overbury, V. Schwartz, D.R. Mullins, W. Yana, S. Dai, J. Catal. 241 (2006) 56–65.
[26] L. Guczi, G. Pető, A. Beck, Z. Pászti, Top. Catal. 29 (2004) 129–138.
[27] G. Pető, G.L. Molnár, Z. Pászti, O. Geszti, A. Beck, L. Guczi, Mater. Sci. Eng. C 19 (2002) 95–99.
[28] G. Pető, O. Geszti, G. Cs. Molnár, S. Daróczi, A. Karacs, L. Guczi, A. Beck, K. Frey, Mater. Sci. Eng. C 23 (2003) 733–736.